RSC Advances

PAPER

View Article Online
View Journal | View Issue

Check for updates

Cite this: *RSC Adv.*, 2021, **11**, 3681

Highly efficient titanosilicate catalyst Ti-MCM-68 prepared using a liquid-phase titanium source for the phenol oxidation†

Satoshi Inagaki, Ryo Ishizuka, Yuya Ikehara, Shota Odagawa, Kai Asanuma, Shunsuke Morimoto and Yoshihiro Kubota *

Received 29th November 2020
Accepted 29th December 2020

DOI: 10.1039/d0ra10081a

rsc.li/rsc-advances

A highly efficient Ti-MCM-68 catalyst for phenol oxidation with H_2O_2 was prepared by a mild liquid-phase treatment for the first time. The key preparation procedures to excellent catalytic activity and high *para*-selectivity were the use of aqueous solutions of the Ti source and calcination at 650 °C prior to catalytic use.

Open Access Article. Published on 18 January 2021. Downloaded on 12/9/2025 10:27:59 AM.
This article is licensed under a Creative Commons Attribution-NonCommercial 3.0 Unported Licence.

Selective oxidation reactions are commonly required for the production of a wide variety of useful chemical compounds, such as highly functional resins and pharmaceuticals. From the view of green sustainable chemistry, hydrogen peroxide (H_2O_2) is well known as one of the most useful oxidants, although its oxidizability is not as strong as ozone (O_3) or peroxycarboxylic acids (*i.e.*, peroxyacetic acid and *m*-chloroperoxybenzoic acid). A titanosilicate catalyst can activate H_2O_2 using selective oxidation to provide indispensable chemical resources.[1]

A wide variety of microporous titanosilicates with isolated tetrahedral Ti species in the zeolitic framework have been developed as catalysts for selective oxidation with H_2O_2.[2–6] For example, TS-1 with MFI topology having multi-dimensional 10-ring channels is an industrially useful titanosilicate that is an effective catalyst for phenol oxidation with H_2O_2 to hydroquinone (HQ), *para*-benzoquinone (*p*-BQ) and catechol (CL) (Scheme 1). Improvement of *para*-selectivity in phenol oxidation over the TS-1 catalyst has been achieved through post-synthetic modification of TS-1 (ref. 7 and 8) or with the aid of a solvent in the reaction system.[7–9]

However, there are significant diffusion limitations for a phenol molecule within the 10-ring straight channel of TS-1 (0.51 × 0.55 nm),[10] although breathing of the pore window could make the aperture expand momentarily. More recently, we have succeeded in the first preparation of Ti-MCM-68 (ref. 11) with MSE-type framework as phenol oxidation catalysts with high activity and selectivity toward HQ. The 12-ring aperture (0.64 × 0.68 nm)[10] in Ti-MCM-68 (ref. 11–13) allowed a phenol molecule to diffuse and preferentially form *para*-isomers.

Although the MSE-type aluminosilicate is hydrothermally synthesized using *N*,*N*,*N*′,*N*′-tetraethyl-bicyclo[2.2.2]oct-7-ene-2,3:5,6-dipyrrolidinium diiodide, $TEBOP^{2+}(I^-)_2$ (ref. 14–26) or dimethyl-dipropylammonium hydroxide[27] as the organic structure-directing agent (OSDA), the direct crystallization of MSE containing framework heteroatoms such as Ti has remained difficult.[28] This is why we are focusing on the isomorphous substitution of Ti for Al in the aluminosilicates, which is a useful technique to introduce a sufficient amount of Ti into the framework.[29] Our first efficient successful way to the preparation of Ti-MCM-68 involved the dealumination by acid treatment followed by gas-phase Ti insertion using $TiCl_4$ at temperatures as high as 600 °C.[11,12] However, the intense reactivity of $TiCl_4$ with moisture, even at room temperature, is a serious issue during this Ti insertion treatment. Therefore, a gentle Ti modification process in the liquid phase at room temperature is desirable. Here we report the first successful preparation of Ti-MCM-68 through treatment at room temperature using an aqueous solution of Ti-source, and its excellent catalytic performance in the phenol oxidation with H_2O_2.

Al-MCM-68 was hydrothermally synthesized according to the known procedures[16–26] (see also ESI†). The crystallinity of MCM-68 samples prepared in this study remained unchanged during calcination, as confirmed by powder X-ray diffraction (Fig. S1†). According to FE-SEM images in Fig. S2,† the MCM-68 particle has a rectangular morphology with 50–80 nm in size. The dealumination treatment of the parent MCM-68 (Si/Al = 10)

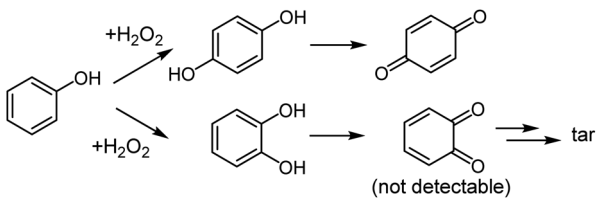

Scheme 1 Reaction pathways of the oxidation of phenol with H_2O_2 to hydroquinone (HQ) and catechol (CL) and subsequent reactions.

Division of Materials Science and Chemical Engineering, Yokohama National University, 79-5 Tokiwadai, Hodogaya-ku, Yokohama 240-8501, Japan. E-mail: kubota-yoshihiro-sr@ynu.ac.jp

† Electronic supplementary information (ESI) available. See DOI: 10.1039/d0ra10081a

© 2021 The Author(s). Published by the Royal Society of Chemistry

Open Access Article. Published on 18 January 2021. Downloaded on 12/9/2025 10:27:59 AM.
This article is licensed under a Creative Commons Attribution-NonCommercial 3.0 Unported Licence.

using concentrated nitric acid solution (13.4 mol L^{-1}) under reflux condition gave highly dealuminated MCM-68 (Si/Al > 1000) without any loss of crystallinity. The dealuminated MCM-68 inevitably had site defects within the MSE framework due to dealumination from the framework (*vide infra*). To introduce Ti into the site defects (*i.e.*, framework), commercially available "titanium(IV) chloride aqueous solution" (Wako Chemical) was used as a reagent. This is a clear yellowish and viscous solution that was prepared by reacting $TiCl_4$ with excess water, and the analytical data were guaranteed as follows: Ti, 3.45 mmol g^{-1}; Cl, 8.18–9.32 mmol g^{-1}. The reaction of $TiCl_4$ with excess H_2O ideally gives a solution with a Cl/Ti molar ratio of 4; however, analytical data showed a lower value of Cl/Ti = 2.37–2.70, which indicates that some HCl was evaporated before the final solution was obtained. This aqueous solution consists of H^+, Cl^-, and Ti^{4+} with various ligands such as H_2O (see next paragraph for more detailed discussion). The concentration of Ti^{4+} was defined; therefore, the aqueous solution was designated as Ti^{4+}/H_2O in this paper. Elemental analysis showed that a sufficient amount of Ti (0.20–0.22 mmol-Ti g^{-1}) was introduced into the dealuminated MCM-68 by treatment with the Ti^{4+}/H_2O. The as-prepared sample to which Ti was introduced at room temperature (16–20 °C) or x °C was denoted as Ti-MCM-68_Ti^{4+}/H_2O_rt or Ti-MCM-68_Ti^{4+}/H_2O_x, respectively. The sample after further thermal treatment (= calcination) at 650 °C is represented by adding "cal" at the end of the sample name (*e.g.* Ti-MCM-68_Ti^{4+}/H_2O_rt_cal). Sorption experiments suggested no diminution in the microporosity or formation of mesopores for Ti-MCM-68_Ti^{4+}/H_2O_rt_cal (Fig. S3 and Table S1†).

Raman spectroscopy is one of the most informative techniques for evaluation of the coordination and conformation of Ti–ligand complexes.[30–36] Fig. 1 shows Raman spectra for the Ti^{4+}/H_2O, neat $TiCl_4$, and $TiCl_4$ dissolved in toluene ($TiCl_4$/toluene). Fig. 1b shows that the $TiCl_4$ molecule gives a sharp peak at 379 cm^{-1}, which corresponds to the $\nu_1(a_1)$ mode,[30,31] accompanied by three peaks at 110 (ν_1(e)), 131 ($\nu_4(f_2)$), and 477 cm^{-1} ($\nu_3(f_2)$).[30,31] The Raman scattering of $TiCl_4$/toluene (Fig. 1c) closely resembled a combination of the two scatterings for neat $TiCl_4$ (Fig. 1b) and toluene (Fig. 1d), which indicates that $TiCl_4$ molecules were intact in the toluene solution without dissociation. In contrast, the Raman peaks of Ti^{4+}/H_2O (Fig. 1a) were entirely different from that of neat $TiCl_4$. A broad band at 650 cm^{-1} and weak broad bands at 150, 340, 460, 790 and 934 cm^{-1} were assignable to $[Ti(OH_2)_6]^{4+}$ octahedra with considerable aggregation.[35] In addition, very weak peaks at 248 and 340 cm^{-1} could correspond to the incorporation of chloride in the first coordination sphere of titanium; possibly, $(TiCl_6)^{2-}$ (O_h) and *trans*-$[Ti(OH_x)_2Cl_4]^{-4+2x}$ (D_{4h}) complexes.[35,36] During this process, it is reasonable to speculate that H_2O and framework oxygens behave as ligands for Ti^{4+}. The Ti^{4+} ions diffuse into the 12-ring channels with repetitive ligand exchange to fill in a site defect of the silicate framework. The possibility of $TiCl_4$ molecule diffusion into the channels was excluded for the following reason. The diameter of the $TiCl_4$ molecule is estimated to be *ca.* 7.4 nm, while that of the 12-ring pore-mouth of MCM-68 is 0.64 × 0.68 nm.[10] It is at least obvious that the $TiCl_4$ molecule cannot enter into the 12-ring channels at temperatures as low as 45 °C. The diffusion of the $[Ti(OH_2)_6]^{4+}$ octahedron itself into the 12-ring channels was also considered to be difficult for the same reason.

Fig. S4† shows DR/UV-vis spectra of various Ti-modified MCM-68 before and after thermal treatment at 650 °C. In the case of Ti^{4+}/H_2O, the as-prepared sample gave a clear peak at 210 nm, which corresponds to a 4-coordinated Ti species at closed sites, $Ti(OSi)_4$, and a shoulder at 250 nm due to 4-coordinated Ti species at open sites, $(OH)Ti(OSi)_3$,[5,29] both of which are inside the framework. This reveals the successful incorporation of tetrahedral Ti into the silicate framework of dealuminated MCM-68 during the suitable treatment at room temperature. After thermal treatment, the UV-vis peak at 210 nm increased slightly, while the UV-vis band at 250 nm remained almost unchanged, which indicates that the dehydration condensation of 4-coordinated Ti with an open site into one of the closed sites with an adjacent silanol proceeded at temperatures as high as 650 °C. In contrast, the treatment of dealuminated MCM-68 using $TiCl_4$/toluene gave different UV-vis bands. There were very broad peaks at 210, 260 and 300 nm, which were attributed to 4-coordinated Ti with the closed site, 5-/6- coordinated Ti, and titanate oligomer, respectively.[5,12,29] The UV-vis band was unchanged even during the thermal treatment at 650 °C, which indicates that $TiCl_4$ molecules did not enter the 12-ring channels of MCM-68 as discussed earlier and may have resulted in partial polymerization on the external surface of dealuminated MCM-68 particles. When using $Ti(OPr^i)_4$/toluene for Ti-impregnation, the resultant sample, which has a large amount of Ti (0.62–0.64 mmol-Ti g^{-1}; see also Table S2†), showed a broad band from 200 to 330 nm. This can be interpreted as the polymerization of titanate species on the external surface of the dealuminated MCM-68 particles. After thermal treatment, the UV-vis band became broader, probably due to the further polymerization of titanate species. Based on these data, only the use of Ti^{4+}/H_2O resulted in the successful introduction of Ti into the MSE framework, and the

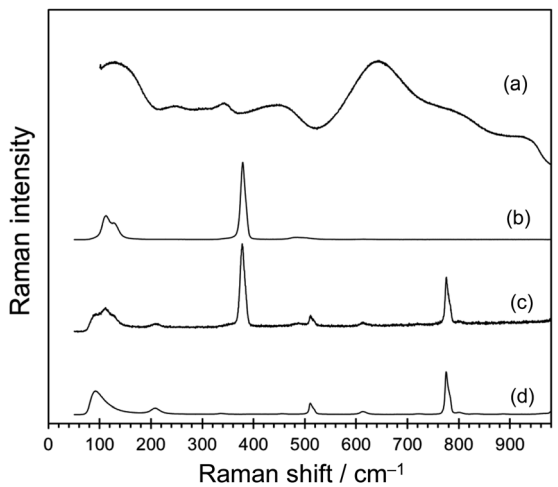

Fig. 1 Raman spectra (532 nm laser) of (a) Ti^{4+}/H_2O obtained by reacting $TiCl_4$ with excess water, (b) neat liquid $TiCl_4$, (c) $TiCl_4$/toluene, and (d) toluene.

© 2021 The Author(s). Published by the Royal Society of Chemistry

Open Access Article. Published on 18 January 2021. Downloaded on 12/9/2025 10:27:59 AM.
This article is licensed under a Creative Commons Attribution-NonCommercial 3.0 Unported Licence.

resultant titanosilicates are potential catalysts for phenol oxidation and related reactions.

The Ti-modified MCM-68 samples were utilized as catalysts for phenol oxidation with H_2O_2 and the results are listed in Table S2.† The Ti-MCM-68 catalyst prepared using $TiCl_4$/toluene (runs 3 and 4) and $Ti(OPr^i)_4$/toluene (run 5) showed only low activity, with or without thermal treatment during the catalyst preparation by liquid-phase Ti-introduction. On the other hand, Ti-MCM-68_Ti^{4+}/H_2O (Table S2,† run 1) exhibited a meaningful product yield (8.7%) with subtle *para*-selectivity (51.7%). This behaviour clearly shows the potential of the preparation methodology with mild treatment conditions using Ti^{4+}/H_2O at room temperature, and strongly supports the spectroscopic results suggesting the incorporation of 4-coordinated Ti species into the MSE framework with such a mild treatment. The reaction over Ti-MCM-68_Ti^{4+}/H_2O_cal obtained after thermal treatment at 650 °C (Table S2,† run 2) gave significantly enhanced total yield (44.4%), turnover number (TON = 478) and *para*-selectivity (81.5%); the catalytic performance became much higher than that of a conventional catalyst, TS-1 (Table S2,† run 6). The significant improvement in the catalytic performance *via* thermal treatment is consistent with the results in our previous reports on Ti-MCM-68 to which Ti was introduced by vapor-phase $TiCl_4$ treatment.[11,12] Note that the remarkable effect of thermal treatment at 650 °C was also represented in Table 1, runs 1 and 2. Such a thermal treatment played some role to increase the hydrophobicity of the titanosilicate catalyst, as proven by the H_2O adsorption isotherm obtained at 25 °C (Fig. 2). The hydrophilic nature of as-prepared Ti-MCM-68_Ti^{4+}/H_2O could be mainly due to connectivity defects (a hydrolysed form of siloxane, ≡Si–OH HO–Si≡, not a silanol nest) in the zeolite framework. Conversely, the reverse process is the condensation of silanols (the reverse process of the siloxane hydrolysis) to give the siloxane bond (≡Si–O–Si≡), and this is considered to be the main cause of hydrophobization during the thermal treatment. The decrease in the number of silanols during the thermal treatment is also supported by ^{29}Si MAS NMR (see Fig. S5†); the spectrum of thermally treated sample had a Q^3 : Q^4 ratio of 6.9 : 93.1, while that of as-prepared sample had a Q^3 : Q^4 ratio of 10.2 : 89.8 (Q^3, HO$\underline{Si}(OSi)_3$; Q^4, $\underline{Si}(OSi)_4$). The enhanced hydrophobicity of Ti-MCM-68 caused an increase

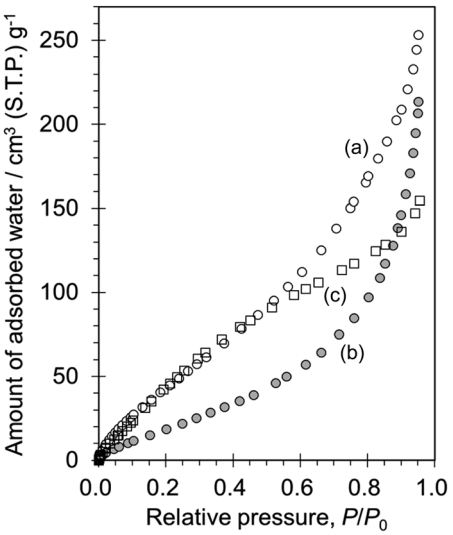

Fig. 2 Water adsorption isotherms obtained at 25 °C for (a) [Ti]-MCM-68_rt_Ti^{4+}/H_2O, (b) [Ti]-MCM-68_rt_Ti^{4+}/H_2O_cal, and (c) TS-1.

in the TON by allowing both phenol and H_2O_2 molecules to simultaneously move into the 12-ring channels.

The influence of the treatment temperature on the Ti modification was examined and the results are shown in Table 1, runs 2, 3, and 4. The temperature was precisely controlled using an oil bath. The Ti^{4+}/H_2O treatment at 25 °C enabled the effective formation of catalytic active sites in the 12-ring channels, and Ti-MCM-68_Ti^{4+}/H_2O_25_cal (Table 1, run 2) exhibited a very high TON (832) and *para*-selectivity (76%). In the case of Ti-MCM-68_Ti^{4+}/H_2O_40_cal and Ti-MCM-68_Ti^{4+}/H_2O_60_cal, TON decreased slightly, probably due to the excess Ti species in the catalyst (Table 1, runs 3 and 4). Such a high-temperature treatment resulted in the polymerization of titanate species on the external surface, as confirmed by the appearance of a broad band at 210–300 nm in the UV-vis spectra (Fig. S6c and f†), although the total yield and *para*-selectivity were still high, despite this negative effect.

The effect of the alcoholic cosolvent[12] was examined, and a typical behaviour is demonstrated in Fig. S7.† The cosolvent here should be recognized as an additive rather than just

Table 1 Oxidation of phenol with H_2O_2 over various titanosilicates[a]

Run	Catalyst	Temperature for Ti-introduction[b]/°C	Ti content[c]/mmol g^{-1}	TON[d]	Yield[e]/%				*para*-Selectivity[f]/%
					Total	HQ	CL	*p*-BQ	
1	Ti-MCM-68_Ti^{4+}/H_2O_25	25	0.206	121	11.4	5.1	4.4	1.8	61.2
2	Ti-MCM-68_Ti^{4+}/H_2O_25_cal	25	0.214	832	88.9	58.9	21.0	9.0	76.3
3	Ti-MCM-68_Ti^{4+}/H_2O_40_cal	40	0.283	667	88.4	59.8	21.3	7.3	75.9
4	Ti-MCM-68_Ti^{4+}/H_2O_60_cal	60	0.439	458	95.8	55.6	27.5	12.7	71.3
5	Ti-MCM-68_cal[g]	600	0.241	314	35.0	26.2	7.6	1.2	78.3

[a] Reaction conditions: catalyst, 20 mg; phenol, 21.25 mmol; H_2O_2, 4.25 mmol, H_2O, 17.9 mmol; temperature, 100 °C; time, 10 min. [b] The treatment with the liquid-phase titanium source was performed at predetermined temperature for 1 h. [c] The Ti content per a gram-catalyst was determined by ICP-AES analysis. [d] Turnover number = (moles of [HQ + CL + *p*-BQ] per mole of Ti site). [e] Product yields based on added H_2O_2. [f] Selectivity to *para*-isomers of dihydroxybenzenes and quinones (moles of [HQ + *p*-BQ] per moles of [HQ + CL + *p*-BQ]). [g] The Ti-modification was performed using vapor-phase $TiCl_4$.

© 2021 The Author(s). Published by the Royal Society of Chemistry

Open Access Article. Published on 18 January 2021. Downloaded on 12/9/2025 10:27:59 AM.
This article is licensed under a Creative Commons Attribution-NonCommercial 3.0 Unported Licence.

a solvent. In the current catalytic system, ethanol (EtOH) was the most suitable cosolvent, which remarkably enhanced *para*-selectivity up to 94%. The role of EtOH could be narrowing the space inside pores and deactivating the external active sites *via* hydrogen bonding between alcoholic OH and surface silanol groups.[12] It should be noted that the use of EtOH as a cosolvent inhibited the production of *p*-BQ, which could be due to the avoidance of radicalic active site formation for the interconversion between HQ and *p*-BQ.

In summary, we have developed a novel and convenient post-synthetic modification procedure for the preparation of Ti-MCM-68 as a highly efficient catalyst for the oxidation of phenol with H_2O_2 for the first time. In this procedure, the Ti^{4+}/H_2O plays an important role to provide Ti^{4+} species to successfully incorporate Ti into the site defects at a temperature as low as room temperature. The improvement of the hydrophobic nature of the catalyst is the most likely factor for the enhanced catalytic performance. Addition of EtOH as a cosolvent to the reaction system realised extremely high selectivity toward HQ. This novel post-synthetic procedure that employs metal chloride aqueous solution under ambient conditions is applicable for the sustainable preparation of efficient catalysts with a wide variety of zeolitic framework.

Conflicts of interest

There are no conflicts to declare.

Acknowledgements

This work was financially supported by the Japan Science and Technology Agency (JST) for the CONCERT-Japan program (Grant Number JPMJSC18C4).

References

1 J. H. Clark, *Green Chem.*, 1999, **1**, 1.
2 B. Notari, *Adv. Catal.*, 1996, **41**, 253–334.
3 T. Tatsumi, *Curr. Opin. Solid State Mater. Sci.*, 1997, **2**, 76–83.
4 I. W. C. E. Arends and R. A. Sheldon, *Appl. Catal.*, 2001, **212**, 175–187.
5 P. Ratnasamy, D. Srinivas and H. Knözinger, *Adv. Catal.*, 2004, **48**, 1.
6 P. Wu and T. Tatsumi, *Catal. Surv. Asia*, 2004, **8**, 137–148.
7 U. Wilkenhöner, G. Langhendries, F. van Laar, G. V. Baron, D. W. Gammon, P. A. Jacobs and E. van Steen, *J. Catal.*, 2001, **203**, 201–212.
8 U. Wilkenhöner, W. L. Duncan, K. P. Möller and E. van Steen, *Microporous Mesoporous Mater.*, 2004, **69**, 181–186.
9 T. Yokoi, P. Wu and T. Tatsumi, *Catal. Commun.*, 2003, **4**, 11–15.
10 C. Baerlocher, L. B. McCusker and D. H. Olson, *Atlas of Zeolite Framework Types*, Elsevier, Amsterdam, 6th edn, 2007, see also: http://www.iza-structure.org/databases/.
11 Y. Kubota, Y. Koyama, T. Yamada, S. Inagaki and T. Tatsumi, *Chem. Commun.*, 2008, **46**, 6224–6226.
12 S. Inagaki, Y. Tsuboi, M. Sasaki, K. Mamiya, S. Park and Y. Kubota, *Green Chem.*, 2016, **18**, 735–741.
13 Y. Ikehara, Y. Ohno, S. Inagaki and Y. Kubota, *Chem. Lett.*, 2017, **46**, 1842–1845.
14 D. C. Calabro, J. C. Cheng, R. A. Crane Jr, C. T. Kresge, S. S. Dhingra, M. A. Steckel, D. L. Stern and S. C. Weston, *US Pat.*, 6049018, 2000.
15 D. L. Dorset, S. C. Weston and S. S. Dhingra, *J. Phys. Chem. B*, 2006, **110**, 2045–2050.
16 T. Shibata, S. Suzuki, H. Kawagoe, K. Komura, Y. Kubota, Y. Sugi, J.-H. Kim and G. Seo, *Microporous Mesoporous Mater.*, 2008, **116**, 216–226.
17 T. Shibata, H. Kawagoe, H. Naiki, K. Komura, Y. Kubota and Y. Sugi, *J. Mol. Catal. A: Chem.*, 2009, **297**, 80–85.
18 S. Ernst, S. P. Elangovan, M. Gerstner, M. Hartmann, T. Hecht and S. Sauerbeck, *Stud. Surf. Sci. Catal.*, 2004, **154C**, 2861–2868.
19 S. Inagaki, K. Takechi and Y. Kubota, *Chem. Commun.*, 2010, **46**, 2662–2664.
20 Y. Kubota, S. Inagaki and K. Takechi, *Catal. Today*, 2014, **226**, 109–116.
21 S. Inagaki, Y. Tsuboi, Y. Nishita, T. Syahylah, T. Wakihara and Y. Kubota, *Chem.–Eur. J.*, 2013, **19**, 7780–7786.
22 Y. Kubota, K. Itabashi, S. Inagaki, Y. Nishita, R. Komatsu, Y. Tsuboi, S. Shinoda and T. Okubo, *Chem. Mater.*, 2014, **26**, 1250–1259.
23 Y. Kubota and S. Inagaki, *Top. Catal.*, 2015, **58**, 480–493.
24 S. Park, Y. Watanabe, Y. Nishita, T. Fukuoka, S. Inagaki and Y. Kubota, *J. Catal.*, 2014, **319**, 265–273.
25 S. Park, S. Inagaki and Y. Kubota, *Catal. Today*, 2016, **265**, 218–224.
26 Q. Han, K. Enoeda, S. Inagaki and Y. Kubota, *Chem. Lett.*, 2017, **46**, 1434–1437.
27 J. G. Moscoso and D. Y. Jan, *US Pat.*, 7922997, 2011.
28 Y. Koyama, T. Ikeda, T. Tatsumi and Y. Kubota, *Angew. Chem., Int. Ed.*, 2008, **47**, 1042–1046.
29 M. Sasaki, Y. Sato, Y. Tsuboi, S. Inagaki and Y. Kubota, *ACS Catal.*, 2014, **4**, 2653–2657.
30 M. F. A. Dove, J. A. Creighton and L. A. Woodward, *Spectrochim. Acta*, 1962, **18**, 267–270.
31 R. J. H. Clark and P. D. Mitchell, *J. Chem. Soc., Faraday Trans. 2*, 1975, **71**, 515–524.
32 D. M. Adams and D. C. Newton, *J. Chem. Soc. A*, 1968, **9**, 2262–2263.
33 J. E. D. Davies and D. A. Long, *J. Chem. Soc. A*, 1968, **10**, 2560–2564.
34 H. F. Shurvell, *J. Mol. Spectrosc.*, 1971, **38**, 431–436.
35 V. D. Hildenbrand, H. Fuess, G. Pfaff and P. Reynders, *Z. Phys. Chem.*, 1996, **194**, 139–150.
36 L. Wang and T. A. Egerton, *Mater. Chem. Phys.*, 2014, **147**, 684–690.

© 2021 The Author(s). Published by the Royal Society of Chemistry